Data in brief 28 (2020) 104889

Contents lists available at ScienceDirect

Data in brief

journal homepage: www.elsevier.com/locate/dib

Data Article

Data on vibrational spectra of the langasites $Ln_3CrGe_3Be_2O_{14}$ (Ln = La, Pr, Nd) and *ab initio* calculations

Nikolay N. Kuzmin [a], Sergey A. Klimin [a], Boris N. Mavrin [a, 1], Kirill N. Boldyrev [a, *], Vladimir A. Chernyshev [b], Boris V. Mill [c], Marina N. Popova [a]

[a] Institute of Spectroscopy, Russian Academy of Sciences, 108840, Troitsk, Moscow, Russia
[b] Department of Basic and Applied Physics, Ural Federal University, 620002, Ekaterinburg, Russia
[c] Faculty of Physics, M.V. Lomonosov Moscow State University, 119991, Moscow, Russia

ARTICLE INFO

Article history:
Received 14 November 2019
Accepted 19 November 2019
Available online 16 December 2019

Keywords:
New langasites
Infrared and Raman spectra
ab initio calculations
Optimized crystal structures
Calculated frequencies and intensities of IR and Raman modes

ABSTRACT

In "Lattice dynamics and structure of the new langasites $Ln_3CrGe_3Be_2O_{14}$ (Ln = La, Pr, Nd): vibrational spectra and *ab initio* calculations" [1], experimental and calculated results on lattice dynamics of the recently discovered new compounds $La_3CrGe_3Be_2O_{14}$, $Pr_3CrGe_3Be_2O_{14}$, and $Nd_3CrGe_3Be_2O_{14}$ are reported. These compounds belong to the langasite series and constitute a new class of low-dimensional antiferromagnets. The data presented in this article includes IR diffuse transmission spectra of powder samples of $Ln_3CrGe_3Be_2O_{14}$ (Ln = La, Pr, Nd) registered at room temperature with a Bruker 125HR Fourier spectrometer, Raman spectra taken in the backscattering geometry (also at room temperature) with a triple monochromator using the line 514, 5 nm of an argon laser as an excitation, results of the DFT calculations with the B3LYP and PBE0 hybrid functionals on the optimized crystal structures, eigenfrequencies and eigenvectors of the normal vibrational modes. These data can be used to analyse electron-phonon interaction and multiferroic properties of the new langasites and to compare the lattice dynamics of different langasites.

DOI of original article: https://doi.org/10.1016/j.jpcs.2019.109266.
* Corresponding author.
E-mail address: kn.boldyrev@gmail.com (K.N. Boldyrev).
[1] Deceased 16 July 2019.

https://doi.org/10.1016/j.dib.2019.104889

The dataset is available on mendeley data public repository at https://doi.org/10.17632/32grbb4p82.1.

Specifications Table

Subject	Materials Science
Specific subject area	Electronic, Optical and Magnetic Materials
Type of data	Table Figure Text file
How data were acquired	IR spectra were collected in diffuse transmission mode with Bruker 125HR Fourier spectrometer, Raman spectra were collected in the backscattering geometry with a home-made triple monochromator using the line 514, 5 nm of an argon laser as an excitation. The CRYSTAL14 program designed for simulating periodic structures in the MO LCAO approximation was used for DFT *ab initio* calculations. Quasi-relativistic pseudopotentials ECP46MWB, ECP59MWB, and ECP60MWB with corresponding valence basis sets ECPnMWB were taken for La, Pr, and Nd. All-electron basis sets of TZVP type were used for Cr, Ge, Be, and O.
Data format	Raw Analyzed
Parameters for data collection	Spectra were collected on powder samples at room temperature. Calculations were performed within the framework of MO LCAO approach and the density functional theory, by using B3LYP and PBE0 hybrid functionals which takes into account both the local and nonlocal (in the Hartree−Fock formalism) exchange.
Description of data collection	Infrared diffuse transmission spectra were registered with a Bruker 125HR Fourier spectrometer equipped with a DTGS and a liquid-nitrogen-cooled MCT detectors. Raman spectra were collected in the backscattering geometry with a home-made triple monochromator (λ_{excit} = 514,5 nm). The frequencies and eigenvectors of the normal vibrational modes were obtained from *ab initio* calculations. First, the full geometry optimization (atomic positions and all unit-cell parameters) was carried out. Then, the phonon spectrum (at the Γ- point) was calculated for the crystal structure corresponding to the minimum energy.
Data source location	Institute of Spectroscopy, Russian Academy of Sciences, Troitsk, Moscow, Russian Federation 55.464596°N37.297538°E
Data accessibility	Repository name: Mendeley Data Data identification number: 32grbb4p82.1 Direct URL to data: https://doi.org/10.17632/32grbb4p82.1
Related research article	N.N. Kuzmin et al., Lattice dynamics and structure of the new langasites $Ln_3CrGe_3Be_2O_{14}$ (Ln = La, Pr, Nd): vibrational spectra and *ab initio* calculations, Journal of Physics and Chemistry of Solids, In Press

Value of the Data

- These data can be used to compare the lattice dynamics of different langasites.
- These data can be used by researchers working on vibrational and magnetoelastic properties of langasites.
- These data can be used to analyse electron-phonon interaction and multiferroic properties of the new langasites.

1. Data description

The dataset includes 6 text files for our measured infrared (IR) and Raman spectra of $Ln_3CrGe_3Be_2O_{14}$ (Ln = La, Pr, Nd, raw data) [1]. These text files are named by rare-earth (RE) element symbol plus the method used to take the spectrum, e.g., Pr_IR.txt means an IR spectrum of $Pr_3CrGe_3Be_2O_{14}$. Each

text file has two columns which correspond to wave number (unit: cm^{-1}) and IR absorbance or Raman intensity (in arbitrary units). The same data are presented also as Excel files, e.g., Pr_IR.xlsx.

The data of *ab initio* calculations of optimized crystal structures is provided in 5 Excel tables. Table 1 provides the coordinates of atoms in the unit cell for the optimized structures of $Ln_3CrGe_3Be_2O_{14}$ (Ln = La, Pr, Nd), calculated with the B3LYP hybrid functional. Table 2 provides the interatomic distances for the optimized structures of $Ln_3CrGe_3Be_2O_{14}$ (Ln = La, Pr, Nd), calculated with the B3LYP hybrid functional. Table 3 provides the lattice constants for the optimized structures of $Ln_3CrGe_3Be_2O_{14}$

Table 1
Calculated (B3LYP) coordinates of atoms in the unit cell of $Ln_3CrGe_3Be_2O_{14}$ (Ln = La, Pr, Nd). The experimental data for $Ln_3CrGe_3Be_2O_{14}$ [14] are shown in square brackets.

Ion	site	Ln = La			Ln = Pr			Ln = Nd		
		x/*a*	*y*/*b*	*z*/*c*	*x*/*a*	*y*/*b*	*z*/*c*	*x*/*a*	*y*/*b*	*z*/*c*
Ln	3*e*	0.42858 [0.42983(4)]	0.	0.	0.42797	0.	0.	0.42776	0.	0.
Cr	1*a*	0.	0.	0.	0.	0.	0.	0.	0.	0.
Ge	3*f*	0.74264 [0.74350(8)]	0.	0.5	0.74243	0	0.5	0.74235	0.	0.5
Be	2*d*	1/3	2/3	0.52202 [0.5260(10)]	1/3	2/3	0.52576	1/3	2/3	0.52735
O1	2*d*	1/3	2/3	0.20577 [0.1973(9)]	1/3	2/3	0.20729	1/3	2/3	0.20790
O2	6*g*	0.46708 [0.4671(4)]	0.30292 [0.3049(3)]	0.32707 [0.3251(5)]	0.46748	0.30543	0.32133	0.46770	0.30667	0.31882
O3	6*g*	0.22247 [0.2256(3)]	0.09505 [0.0966(3)]	0.75926 [0.7571(4)]	0.22352	0.09250	0.75799	0.22402	0.09133	0.75743

Table 2
Calculated (B3LYP) and experimentally determined [14] (in square brackets) M − O distances (Å) in the structure of $Ln_3CrGe_3Be_2O_{14}$ (Ln = La, Pr, Nd).

	Ln = La	Ln = Pr	Ln = Nd
R−polyhedron			
R−O1 × 2	2.637 [2.577(2)]	2.621	2.613
R−O2 × 2	2.520 [2.457(4)]	2.473	2.451
R−O2′ × 2	2.850 [2.816(3)]	2.827	2.818
R−O3 × 2	2.488 [2.450(3)]	2.449	2.431
$(R-O)_{av}$	2.624 [2.575]	2.593	2.578
Cr−octahedron			
Cr−O3 × 6	1.987 [1.979(2)]	1.984	1.983
Ge− tetrahedron			
Ge−O2 × 2	1.784 [1.760(4)]	1.781	1.780
Ge−O3 × 2	1.774 [1.733(3)]	1.775	1.775
$(Ge-O)_{av}$	1.779 [1.747]	1.778	1.778
Be−tetrahedron			
Be−O1	1.586 [1.622(6)]	1.589	1.590
Be−O2 × 3	1.698 [1.672(3)]	1.694	1.692
$(Be-O)_{av}$	1.670 [1.660]	1.668	1.667

Table 3
Experimentally determined [14] and calculated (PBE0) lattice constants (Å) of $Ln_3CrGe_3Be_2O_{14}$.

$Ln_3CrGe_3Be_2O_{14}$		a	c
$La_3CrGe_3Be_2O_{14}$	Exp.	8.033(2)	4.934(2)
	Calc.	8.0622	4.9680
$Pr_3CrGe_3Be_2O_{14}$	Exp.	7.957(2)	4.904(2)
	Calc.	7.9968	4.9433
$Nd_3CrGe_3Be_2O_{14}$	Exp.	7.931(2)	4.894(2)
	Calc.	7.9683	4.9323

(Ln = La, Pr, Nd), calculated with the PBE0 hybrid functional. Table 4 provides the coordinates of atoms in the unit cell for the optimized structures of $Ln_3CrGe_3Be_2O_{14}$ (Ln = La, Pr, Nd), calculated with the PBE0 hybrid functional. Table 5 provides the interatomic distances for the optimized structures of $Ln_3CrGe_3Be_2O_{14}$ (Ln = La, Pr, Nd), calculated with the PBE0 hybrid functional. In Tables 1–5, available experimental data are in square brackets.

The dataset includes 3 text files for the calculated with the B3LYP hybrid functional frequencies of normal modes and their intensities in the IR and Raman spectra. These text files are named by RE element symbol plus the method to get the data, e.g., Pr_abinit.txt means the calculated data for $Pr_3CrGe_3Be_2O_{14}$. Each text file has four columns which correspond to the symmetry of the mode (irreducible representation), wave number (unit: cm^{-1}), IR intensity, Raman intensity (arb. units). First, all A_1 modes are listed, they are followed by the A_2 and, then, E modes. The same data are presented also as Excel files, e.g., Pr_abinit.xlsx. Three Excel Tables, Table 6, Table 7, and Table 8**,** provide all calculated modes compared with those found from the measured spectra (analyzed data), in increasing order of their frequency for $La_3CrGe_3Be_2O_{14}$, $Pr_3CrGe_3Be_2O_{14}$, and $Nd_3CrGe_3Be_2O_{14}$, respectively. Mode symmetries are indicated.

The data on calculated displacements of different atoms in normal crystal modes of different frequencies for $Ln_3CrGe_3Be_2O_{14}$ (Ln = La, Pr, Nd) is provided in 3 text files named, e.g., Pr_displ.txt. Each

Table 4
Calculated (PBE0) and experimentally determined [14] (in square brackets) coordinates of atoms in the unit cell of $Ln_3CrGe_3Be_2O_{14+}$ (Ln = La, Pr, Nd).

Ion	site	Ln = La			Ln = Pr			Ln = Nd		
		x/*a*	*y*/*b*	*z*/*c*	*x*/*a*	*y*/*b*	*z*/*c*	*x*/*a*	*y*/*b*	*z*/*c*
Ln	3*e*	0.43071 [0.42983(4)]	0	0	0.43021	0	0	0.42976	0	0
Cr	1*a*	0	0	0	0	0	0	0	0	0
Ge	3*f*	0.74464 [0.74350(8)]	0	0.5	0.74435	0	0.5	0.74428	0	0.5
Be	2*d*	1/3	2/3	0.52203 [0.5260(10)]	1/3	2/3	0.52539	1/3	2/3	0.52713
O1	2*d*	1/3	2/3	0.20488 [0.1973(9)]	1/3	2/3	0.20613	1/3	2/3	0.20711
O2	6*g*	0.46553 [0.4671(4)]	0.30026 [0.3049(3)]	0.32701 [0.3251(5)]	0.46600	0.30279	0.32134	0.46618	0.30408	0.31883
O3	6*g*	0.22215 [0.2256(3)]	0.09317 [0.0966(3)]	0.75867 [0.7571(4)]	0.22329	0.09093	0.75757	0.22364	0.08958	0.75679

Table 5
Calculated (PBE0) and experimentally determined [14] (in square brackets) M − O distances (Å) in the structure of $Ln_3CrGe_3Be_2O_{14}$ (Ln = La, Pr, Nd).

	Ln = La	Ln = Pr	Ln = Nd
R−polyhedron			
R−O1 × 2	2.601 [2.577(2)]	2.584	2.578
R−O2 × 2	2.496 [2.457(4)]	2.449	2.429
R−O2′ × 2	2.811 [2.816(3)]	2.788	2.779
R−O3 × 2	2.468 [2.450(3)]	2.430	2.412
$(R-O)_{cp}$	2.594 [2.575]	2.563	2.550
Cr−octahedron			
Cr−O3 × 6	1.966 [1.979(2)]	1.963	1.963
Ge− tetrahedron			
Ge−O2 × 2	1.769 [1.760(4)]	1.766	1.764
Ge−O3 × 2	1.756 [1.733(3)]	1.756	1.756
$(Ge-O)_{cp}$	1.762 [1.747]	1.761	1.760
Be−tetrahedron			
Be−O1	1.576 [1.622(6)]	1.578	1.579
Be−O2 × 3	1.683 [1.672(3)]	1.678	1.677
$(Be-O)_{cp}$	1.656 [1.660]	1.653	1.653

Table 6
Experimentally determined [1] and calculated (B3LYP) frequencies in the Raman (R) and infrared (IR) spectra of $La_3CrGe_3Be_2O_{14}$.

Exp, R	Calculated			Exp, IR	Exp, R	Calculated			Exp, IR
	A1	E	A2			A1	E	A2	
Raman – active					Raman – active				
		IR – active					IR – active		
			88					396	400
108		105		100	406	396			
108		109			433		425		424
122	127				462		456		456
			130	133	488		482		
143		141						499	506
			156		544		532		551
159		164		167	568	561			
190		193		189				580	
	212				586	583			
			213	216	625		624		625
233		235					661		
		241		245			715		722
259		269		265	730		728		722
	284							733	741
			287		783		781		789
292		290		294	783	785			
292	292						809		
326		328						816	
			332			818			
351		343		344				825	821
378		376		384	836	839			

Table 7
Experimentally determined [1] and calculated (B3LYP) frequencies in the Raman (R) and infrared (IR) spectra of $Pr_3CrGe_3Be_2O_{14}$.

Exp, R	Calculated			Exp, IR	Exp, R	Calculated			Exp, IR
	A1	E	A2			A1	E	A2	
Raman – active					Raman – active				
		IR – active					IR – active		
			83	89				398	404
		96		89	409	401			
108		108			435		431		430
123	127				462		459		462
			131	135	489		485		
145		141						503	509
			150		548		538		556
161		164		166	575	565			
193		194		188				583	
	215				587	587			
			216		631		632		633
235		235					668		
		243		245			721		728
260		265		263				734,5	743
	284				732		734,8		743
			286		783		785,6		794
295		294		297	783	785,7			
295	297						813		
		327				818			
			337					821	823
355		348		352				823	823
382		378		385	836	843			

Table 8
Experimentally determined [1] and calculated (B3LYP) frequencies in the Raman (R) and infrared (IR) spectra of $Nd_3CrGe_3Be_2O_{14}$.

Exp, R	Calculated			Exp, IR	Exp, R	Calculated			Exp, IR
	A1	E	A2			A1	E	A2	
Raman−active					Raman−active				
		IR−active					IR−active		
			80					400	405
		92		90	410	404			
108		108			436		434		435
123	127				463		461		463
			131	138	490		486		
146		141						505	512
			148		549		540		560
160		165		166	572	569			
191		194		191				585	
	217				589	590			
			218		626		635		634
236		236					671		
		244		247			723		731
261		264		265	734			735	746
	284						738		
			286		784	786			794
296		295		301	784		787		794
	301						814		
330		327				817			
			340					820	
356		351		354				826	823
382		380		385	838	845			

text file has eight columns. The first column correspond to the mode frequency (unit: cm^{-1}), the columns 2−8 correspond to the displacements (unit: Å) of the following atoms: Ln, Cr, Ge, Be, O1, O2, O3. The same data are presented also as Excel tables with 8 columns, named, e.g., Pr_displ.xlsx.

Fig. 1 depicts these displacements for all three title compounds, namely, $La_3CrGe_3Be_2O_{14}$, $Pr_3CrGe_3Be_2O_{14}$, and $Nd_3CrGe_3Be_2O_{14}$. It is given as the eps and opj files, Figure 1.eps and Figure 1.opj, respectively. The table in text (and Excel) format Figure 1_table.txt (and Figure 1_table.xlxs) provides the data necessary to create Figure 1.

2. Experimental design, materials, and methods

The main information on the samples and experimental equipment used to take the spectra, as well as on the calculation methods is presented in Ref. [1]. Powder samples of the studied compounds $La_3CrGe_3Be_2O_{14}$, $Pr_3CrGe_3Be_2O_{14}$, and $Nd_3CrGe_3Be_2O_{14}$ were synthesized by a high-temperature solid-state reaction from high-purity La_2O_3, Pr_2O_3, Nd_2O_3 and GeO_2, Cr_2O_3 (reagent grade), and BeO (99.54%). Stoichiometric amounts of oxides were thoroughly ground together, pressed into pellets, placed on a Pt substrate and sintered in air for 5 h at 1350°C (the Nd and Pr compounds) and at 1325°C (the La compound). To reduce the loss of GeO_2 due to evaporation, the pressed samples were encapsulated in the original powdered charges. The phase composition of sintering products was studied by X-ray diffraction using a diffractometer STOE STADI_MP in a transmission mode (Cu$K_{\alpha 1}$ radiation). The space group *P*321 was confirmed for all samples.

The infrared diffuse transmission and Raman scattering spectra of $Ln_3CrGe_3Be_2O_{14}$ (Ln = La, Pr, Nd) powder samples were measured at room temperature. Powders of $Ln_3CrGe_3Be_2O_{14}$ were mixed with optical-grade KBr powder and pressed into pellets. Far-infrared diffuse transmission spectra were registered in the spectral region 50−1200 cm^{-1} at a resolution 2 cm^{-1} using a Fourier spectrometer Bruker IFS 125HR and a DTGS and a liquid-nitrogen-cooled MCT detectors. Raman spectra were taken in the backscattering geometry at a resolution 3 cm^{-1} with a home-made triple monochromator using the line 514, 5 nm of an argon laser as an excitation.

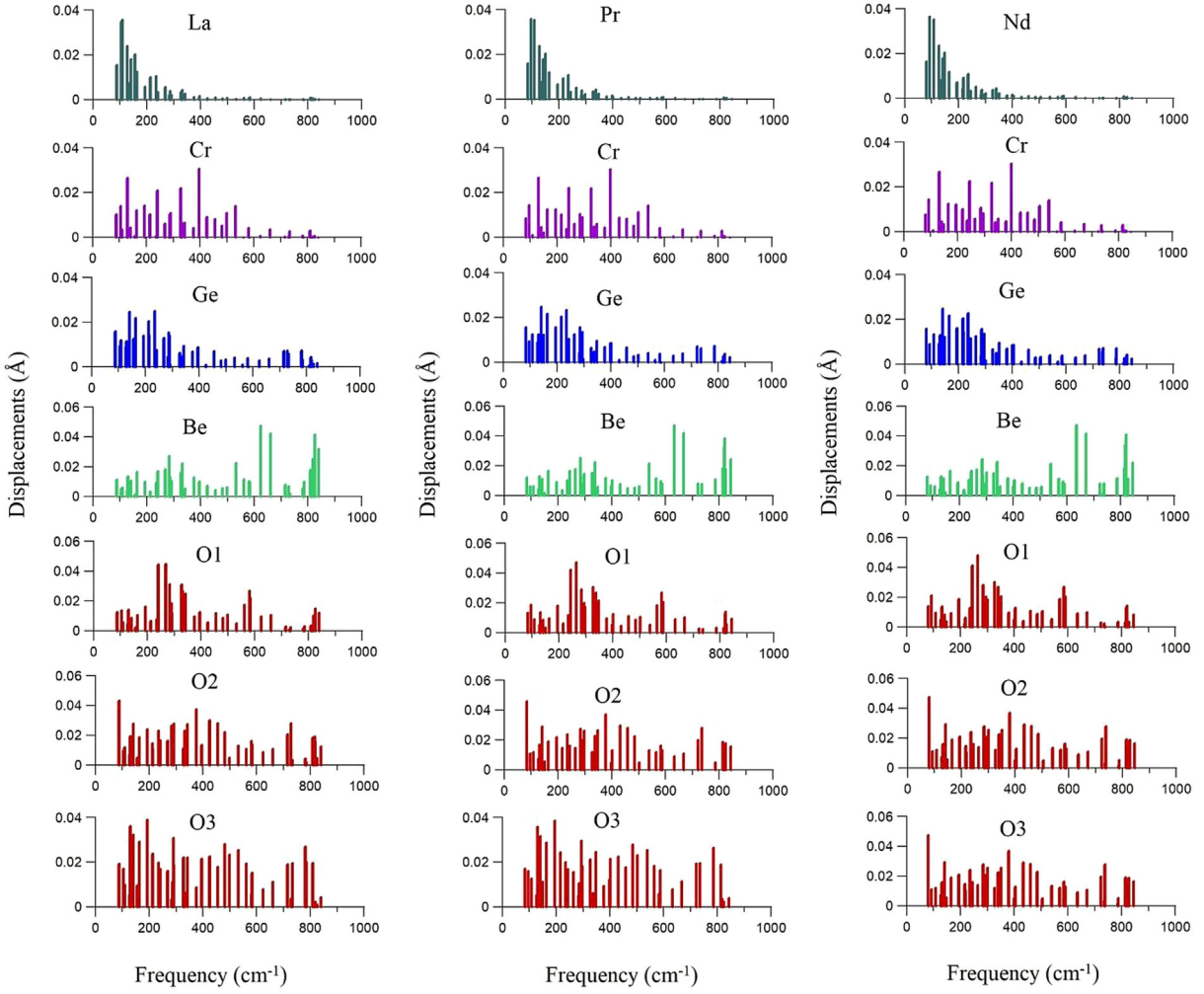

Fig. 1. Displacements of different atoms of $La_3CrGe_3Be_2O_{14}$ in normal crystal modes of different frequencies.

Ab initio calculations of phonon frequencies and intensities of the infrared- and Raman-active modes of $La_3CrGe_3Be_2O_{14}$, $Pr_3CrGe_3Be_2O_{14}$, and $Nd_3CrGe_3Be_2O_{14}$ were performed in a framework of the density functional theory (DFT) with the hybrid functional B3LYP [2], which takes into account both local and nonlocal (in the Hartree-Fock formalism) exchange. The sequence of calculations was as follows. The optimization of the crystal structure was carried out first. After that, the phonon spectrum was calculated for the crystal structure corresponding to the minimum energy. The CRYSTAL14 program [3] designed for simulating periodic structures in the MO LCAO approximation was used for calculations. Quasi-relativistic pseudopotentials ECP46MWB, ECP59MWB, and ECP60MWB [4,5] with corresponding valence basis sets ECP*n*MWB [6] were taken for La, Pr, and Nd. All-electron basis sets of TZVP type were used for Cr, Ge, Be, and O [7]. These basis sets are available at the CRYSTAL website. The reciprocal space sampling was performed by Monkhorst-Pack mesh. The algorithm of calculation of the two-electron Coulomb and exchange integrals is given in Ref. [8]. The tolerance of self-consistently solving of the system of Kohn-Sham equations was 10^{-9}. The phonon spectrum was calculated in the harmonic approximation. In the Hessian matrix, the first (second) derivatives were calculated analytically (numerically). To perform numerical calculations of the second derivatives, the atom was displaced from the equilibrium position by 0.003 Å [8].

We used the Born charges when calculating Raman and infrared intensities in the CRYSTAL code [9]. Electric dipole properties were calculated using the periodic coupled-perturbed Hartree-Fock (CPHF) or Kohn-Sham (CPKS) approach [10–12].

The Placzek approximation was used to calculate the intensity of the Raman modes at a non-resonant excitation [11]. For an oriented single crystal, the intensity associated with the mode ω_k is [3]:

$$I_{ij}^{k} \propto C\left(\alpha_{ij}^{k}\right)^2, \tag{1}$$

where α_{ij}^{k} is an element of the Raman tensor, $i,j = x,y,z$. The value C in (1) is defined by the laser frequency ω_L and the temperature T dependence as follows:

$$C \sim \frac{1+n(\omega_k)}{30\omega_k}(\omega_L - \omega_k)^4, \tag{2}$$

where

$$1+n(\omega_k) = \left[1 - \exp\left(-\frac{\hbar\omega_k}{k_B T}\right)\right]^{-1}, \tag{3}$$

$n(\omega_k)$ being the Bose occupation factor.

The simulation of the intensity of Raman modes for powder sample has been done by computing integrals over all possible orientations of ideal bulk crystal. These integrals can be reduced to three rotational invariants [13]:

$$G_k^{(0)} = \frac{1}{3}\left(\alpha_{xx}^{k} + \alpha_{yy}^{k} + \alpha_{zz}^{k}\right)^2 \tag{4}$$

$$G_k^{(1)} = \frac{1}{2}\left[\left(\alpha_{xy}^{k} - \alpha_{yx}^{k}\right)^2 + \left(\alpha_{xz}^{k} - \alpha_{zx}^{k}\right)^2 + \left(\alpha_{zy}^{k} - \alpha_{yz}^{k}\right)^2\right] \tag{5}$$

$$\begin{aligned} G_k^{(2)} = {} & \frac{1}{2}\left[\left(\alpha_{xy}^{k} + \alpha_{yx}^{k}\right)^2 + \left(\alpha_{xz}^{k} + \alpha_{zx}^{k}\right)^2 + \left(\alpha_{zy}^{k} + \alpha_{yz}^{k}\right)^2\right] \\ & + \frac{1}{3}\left[\left(\alpha_{xx}^{k} - \alpha_{yy}^{k}\right)^2 + \left(\alpha_{xx}^{k} - \alpha_{zz}^{k}\right)^2 + \left(\alpha_{yy}^{k} - \alpha_{zz}^{k}\right)^2\right] \end{aligned} \tag{6}$$

The intensity for the powder sample can be calculated as [14]:

$$I_{tot,k}^{powder} = I_{\parallel,k}^{powder} + I_{\perp,k}^{powder}, \tag{7}$$

where

$$I_{\parallel,k}^{powder} = C\left(10G_k^{(0)} + 4G_k^{(2)}\right) \tag{8}$$

$$I_{\perp,k}^{powder} = C\left(5G_k^{(1)} + 3G_k^{(2)}\right) \tag{9}$$

and C is given by Eq. (2).

The infrared intensity of the p-th mode can be written as [3]:

$$I_p = \frac{\pi}{3}\frac{N_A}{c^2} d_p \left|\vec{Z}_p\right|^2, \tag{10}$$

where N_A is the Avogadro's number, c is the speed of light, d_p is the degeneracy of the mode, $\vec{Z}_p$ is the mass-weighted Born effective charge vector of the mode. The infrared intensity was calculated assuming an isotropic response.

The high-spin ($S = 3/2$) state of the Cr^{3+} ions was set in the calculations. At the simulation, magnetic moments of chromium ions were codirected (along the z axis), hereby the ferromagnetic state was simulated. In this work, we consecutively calculate the crystal structure and, then, the phonon spectrum. The initial structural data were taken from Ref. [14].

When choosing a functional, calculations with the hybrid functional PBE0 [15] were also performed.

Acknowledgments

This work was supported by the Russian Foundation for Basic Research under Grant #17-02-00603. Optical spectroscopy research was performed on the Unique Scientific Installation of the Institute of Spectroscopy “Multifunctional wide-range high-resolution spectroscopy” (http://www.ckp-rf.ru/usu/508571).

Conflict of Interest

The authors declare that they have no known competing financial interests or personal relationships that could have appeared to influence the work reported in this paper.

Appendix A. Supplementary data

Supplementary data to this article can be found online at https://doi.org/10.1016/j.dib.2019.104889.

References

[1] N.N. Kuzmin, S.A. Klimin, B.N. Mavrin, K.N. Boldyrev, V.A. Chernyshev, B.V. Mill, M.N. Popova, Lattice dynamics and structure of the new langasites Ln3CrGe3Be2O14 (Ln = La, Pr, Nd): vibrational spectra and ab initio calculations, J. Phys. Chem. Solids (2019) 109266, https://doi.org/10.1016/j.jpcs.2019.109266, in press.
[2] A.D. Becke J, Density-functional thermochemistry. III. The role of exact exchange, Chem. Phys. 98 (1993) 5648–5652, https://doi.org/10.1063/1.464913.
[3] R. Dovesi, V.R. Saunders, C. Roetti, R. Orlando, C.M. Zicovich-Wilson, F. Pascale, B. Civalleri, K. Doll, N.M. Harrison, I.J. Bush, Ph D'Arco, M. Llunel, M. Causa, Y. Noel, CRYSTAL14 User's Manual, University of Torino, Torino, 2014.
[4] M. Dolg, H. Stoll, A. Savin, H. Preuss, Energy-adjusted pseudopotentials for the rare earth elements, Theor. Chim. Acta 75 (1989) 173–194, https://doi.org/10.1007/BF00528565.
[5] M. Dolg, H. Stoll, H. Preuss, A combination of quasirelativistic pseudopotential and ligand field calculations for lanthanoid compounds, Theor. Chim. Acta 85 (1993) 441–450, https://doi.org/10.1007/BF01112983.
[6] Energy-consistent Pseudopotentials of the Stuttgart/Cologne Group, 2019, 2019. http://www.tc.uni-koeln.de/PP/clickpse.en.html. (Accessed 27 October 2019).

[7] M.F. Peintinger, D.V. Oliveira, T. Bredow, Consistent Gaussian basis sets of triple-zeta valence with polarization quality for solid-state calculations, J. Comput. Chem. 34 (2013) 451–459, https://doi.org/10.1002/jcc.23153.
[8] F. Pascale, C.M. Zicovich-Wilson, F. Lopez Gejo, B. Civalleri, R. Orlando, R. Dovesi, The calculation of the vibrational frequencies of crystalline compounds and its implementation in the CRYSTAL code, J. Comput. Chem. 25 (2004) 888–897, https://doi.org/10.1002/jcc.20019.
[9] L. Maschio, B. Kirtman, R. Orlando, M. Rerat, *Ab initio* analytical infrared intensities for periodic systems through a coupled perturbed Hartree-Fock/Kohn-Sham method, J. Chem. Phys. 137 (2012) 204113, https://doi.org/10.1063/1.4767438.
[10] L. Maschio, B. Kirtman, M. Rérat, R. Orlando, R. Dovesi, *Ab initio* analytical Raman intensities for periodic systems through a coupled perturbed Hartree-Fock/Kohn-Sham method in an atomic orbital basis. I. Theory, J. Chem. Phys. 139 (2013) 164101, https://doi.org/10.1063/1.4824442.
[11] L. Maschio, B. Kirtman, M. Rérat, R. Orlando, R. Dovesi, *Ab initio* analytical Raman intensities for periodic systems through a coupled perturbed Hartree-Fock/Kohn-Sham method in an atomic orbital basis. II. Validation and comparison with experiments, J. Chem. Phys. 139 (2013) 164102, https://doi.org/10.1063/1.4824443.
[12] R. Orlando, V. Lacivita, R. Bast, K. Ruud, Calculation of the first static hyperpolarizability tensor of three-dimensional periodic compounds with a local basis set: a comparison of LDA, PBE, PBE0, B3LYP, and HF results, J. Chem. Phys. 132 (2010) 244106, https://doi.org/10.1063/1.3447387.
[13] S.A. Prosandeev, U. Waghmare, I. Levin, J. Maslar, First-order Raman spectra of $AB'_{1/2}B''_{1/2}O_3$ double perovskites, Phys. Rev. B 71 (2005) 214307, https://doi.org/10.1103/PhysRevB.71.214307.
[14] B.V. Mill, Z.A. Kazei, D.M. Tsymbarenko, Formation of phases with the $Ca_3Ga_2Ge_4O_{14}$ structure in the systems Ln_2O_3–M_2O_3–GeO_2–BeO (Ln = La–Gd, M = Ga, Al, Fe, Cr), Russ. J. Inorg. Chem. 63 (2018) 1283–1290, https://doi.org/10.1134/S0036023618100133.
[15] J.P. Perdew, M. Ernzerhof, K. Burke, Rationale for mixing exact exchange with density functional approximations, J. Chem. Phys. 105 (1996) 9982–9985, https://doi.org/10.1063/1.472933.